LBL-13619
Conf-821011--31

Lawrence Berkeley Laboratory

UNIVERSITY OF CALIFORNIA

Engineering & Technical Services Division

MASTER

Presented at the 1982 IEEE Nuclear Science Symposium, Washington, DC, October 19-22, 1982

AFTERPULSE TIME-SPECTRUM MEASUREMENT OF RCA 8850 PHOTOMULTIPLIER

C.C. Lo and Branko Leskovar

October 1982

Prepared for the U.S. Department of Energy under Contract DE-AC03-76SF00098

DISTRIBUTION OF THIS DOCUMENT IS UNLIMITED

AFTERPULSE TIME-SPECTRUM MEASUREMENT OF RCA 8850 PHOTOMULTIPLIER

LBL-13619

LBL--13619

DE83 004159

C. C. Lo and Branko Leskovar

Lawrence Berkeley Laboratory
University of California
Berkeley, California 94720

ABSTRACT

The photomultiplier dark pulse-height, signal induced pulse-height, and afterpulse time spectra have been measured on three RCA 8850 52 mm-diameter photomultipliers. The first dynode of this photomultiplier has a cesium activated, gallium-phosphide secondary emitting surface. Measurement techniques and the measuring systems are described in detail.

INTRODUCTION

The RCA 8850 two-inch 12-stage photomultiplier is a modified version of the RCA 8575. Both types have identical eletron multiplier structures, the electron optics and semitransparent cesium-potassium-antimony photocathodes deposited on a pyrex entrance window. The only significant difference between 8850 and 8575 is that 8850 has a cesium-activated gallium-phosphide secondary emitting surface on the first dynode. This surface has a secondary emission ratio of 30-50 instead of 5-8 as does the conventional dynode material. The high pulse-height resolution of the 8850 makes it possible to set the threshold of the signal discriminator in the valley between the single and two-photoelectron peaks, thus eliminating most of the single-photoelectron pulses which are mostly thermionic initiated from the photocathode. This paper presents and discusses new measurements of the photomultiplier dark pulse-height and afterpulse time spectra. Other characteristics of the photomultipliers, generally not available from manufacturers, have been measured and presented previously.[1-3]

Contemporary fabrication and activation techniques have reduced afterpulses from most photomultipliers to a point where they are rarely important. However, for some applications afterpulses still may introduce serious error. For example, in photon counting systems for subnanosecond fluorescence lifetime measurements[4] photomultiplier afterpulses can generate small amplitude late artifactual peaks in the sample fluorescence profile.[5] Also, in Deep Underwater Muon and Neutrino Detection (DUMAND) systems which use a large number of photomultipliers in a three-dimensional array a significant amount of afterpulsing could introduce serious error in measuring particle trajectories.[6,7]

In general, the afterpulses are produced as a result of the ionization of residual gases, such as He^+, H_2^+, N_2^+ and CO^+, in the volume between the photocathode and the first dynode. The positive ions formed are accelerated toward the photocathode by the focusing electric field. On impact these ions liberate up to five secondary electrons which produce an afterpulse signal. These afterpulses generally occur from 20 ns to several microseconds after the main pulse. The time of occurrence of the afterpulses can be closely correlated with the atomic mass of the residual gas inside the glass envelope. This phenomena was studied systematically by several authors[8] who introduced trace amounts of various gasses into photomultipliers. Subsequently, in further work[9-11], the physical origins of afterpulses was investigated, particularly with respect to the afterpulses which result from the diffusion of helium through the photomultiplier glass envelope. Although the helium is present in small concentration in ambient air, it is sufficient so that its atoms, which can permeate readily through the glass envelope, can cause afterpulses. This effect is often enhanced by the fact that photomultipliers are frequently used in laboratories where ambient concentration of helium is significantly increased by the emissions from helium Dewar bottles or from gas Cherenkov counters. Other phenomena may also cause afterpulsing, such as dynode fluorescence, electrical fields over the exposed glass of the envelope, etc. In order to measure this characteristic, a pulse height spectrum, a signal induced pulse-height spectrum and a time spectrum must be taken of the anode output pulses. Measurements were made using the voltage divider network suggested by RCA for fast pulse response. With 2500 V applied between the anode and cathode, the average gain was approximately 1.8×10^6, while the dark current was 4.6×10^{-8} A.

PULSE-HEIGHT SPECTRUM MEASUREMENT

Figure 1 is a block diagram of the system for measuring the pulse-height spectrum.

A pulse generator was used to drive a light-emitting diode, type XP 21. The light intensity of the pulses was controlled by the drive pulse amplitude. The light emitting diode was placed more than one meter away from the photocathode of the photomultiplier. An attenuator and preamplifier was used at the output of the photomultiplier to provide more flexibility for controlling pulse-height spectrum display on the pulse-height analyzer.

Table 1 shows the dark pulse count of the three 8850s from 1/8 photoelectron peak to 16 photoelectrons and also at various photelectron peaks to 16 photoelectron level, inclusive. The most obvious feature was that most of the dark pulses are due to single electron. Only a few percent of the dark pulses consist of two photoelectrons or more. These are probably quite different in origin from the single electron pulse. The dark pulse count of the three 8850s ranges from 204 counts per second to 234 per second by summing all pulses between 1/8 photoelectron to 16 photoelectrons. Figure 2 shows a typical dark pulse-height spectrum of an 8850.

Table 2 shows the results of the high counting rate measurement. For this measurement the light emitting diode was pulsed at 1 MHz and the light level was adjusted so that the 8850 yielded 10^5 of

DISTRIBUTION OF THIS DOCUMENT IS UNLIMITED

DISCLAIMER

This report was prepared as an account of work sponsored by an agency of the United States Government. Neither the United States Government nor any agency thereof, nor any of their employees, makes any warranty, express or implied, or assumes any legal liability or responsibility for the accuracy, completeness, or usefulness of any information, apparatus, product, or process disclosed, or represents that its use would not infringe privately owned rights. Reference herein to any specific commercial product, process, or service by trade name, trademark, manufacturer, or otherwise, does not necessarily constitute or imply its endorsement, recommendation, or favoring by the United States Government or any agency thereof. The views and opinions of authors expressed herein do not necessarily state or reflect those of the United States Government or any agency thereof.

single photoelectron pulses per second. Note that the 100 kHz pulse repetition frequency was limited by the pulse-height analyzer used in the measuring system. Under high, single-photoelectron counting operation the percentage of pulses counted consisting of three photoelectrons or more was smaller than in the dark pulse count case. It appears that this effect is caused by a gain decrease of the photomultiplier operating at the signal induced condition and by statististical error of the measurement. Figure 3 shows a typical pulse-height spectrum of an 8850 under 100 kHz single photoelectron counting operation.

AFTERPULSE MEASUREMENT

The system shown in Fig. 4 was used to measure afterpulses. A pulse generator was used to drive a light-emitting diode, type XP 21, which, produced light pulses for the photomultiplier. The trigger pulse from the pulse generator was delayed and shaped and then used as a start pulse for the time-to-amplitude converter (TAC). The output pulse of the photomultiplier was used as the stop pulse for the TAC after being processed by a constant fraction discriminator. In order to count the afterpulses which came immediately after the main photomultiplier pulse, the main output pulse (marked by symbol B in Fig. 4) was delayed after the start pulse. The time at which the main photomultiplier pulse occurred was taken as time zero. However, in order to count the afterpulses which occurred significantly later in time and with a very low count rate the trigger pulse from the pulse generator was purposely delayed to come after the photomultiplier main pulse so that an output pulse from the TAC would only occur when the photomultiplier generated an afterpulse. The output of the TAC was then recorded and displayed on a pulse-height analyzer. In order to look for pulses many microseconds after the main pulse (the timing range of the TAC being set accordingly) the operating frequency of the test system was quite low. Table 3 shows the results of the afterpulse measurement.

Under single photoelectron counting at a rate of 100 kHz, afterpulses were detected in the time interval ranges of 18-22 ns and 343-415 ns, after the main output pulse in all three photomultipliers. In the 450 ns to 68 μs time range afterpulses were not detected in any of the three photomultipliers.

When the light pulse intensity was increased so that pulses with three photoelectrons were produced by the 8850s, afterpulses were detected in the 19-22 ns, 342-413 ns time intervals as before in all three photomultipliers. Detailed results are given in Table 3.

Figure 5 shows the time distribution of output pulses in logarithmic scale in the time interval 0-150 ns after the main photomultiplier pulse under a 100 kHz single photoelectron counting rate. The first distribution at the beginning of the spectrum is the main output pulse of the photomultiplier. The second distribution represents the afterpulses which occurred 18 ns after the main pulse.

Figure 6 shows the same afterpulse spectrum on a linear time scale over the range 60-680 ns under 100 kHz single-photoelectron counting rate. Afterpulses were also present from 351-415 ns after the main photomultiplier output pulse.

CONCLUSIONS

Measurement on three 8850 photomultipliers show that afterpulses occurred with all three at 18-22 ns and 342-415 ns after the main anode output pulse. No afterpuse was observed beyond this range up to 68 μs under single-photoelectron or three photoelectron operating conditions. Afterpulses in the 342-415 ns range had a peak amplitude of approximately 2-3 times that of the main pulse. The photomultipliers tested were ten years old. During this time they had been mostly used for calibration purposes of various single-photon counting systems and high-gain photon detectors under controlled conditions in a standard laboratory environment.

The afterpulses occurring in the 342-415 ns range were attributed to He^+ ions which are created in the space between the photocathode and the first dynode and the first and second dynode. This conclusion is based on the time-of-flight of the helium ion from its point of origin to the photocathode and the ion mass-to-charge ratio. These afterpulses clearly showed a two peak structure. The first peak of this distribution is caused by afterpulses generated by He^+ ions from the photocathode-first dynode region. The second peak is produced by afterpulses generated by ions which are formed between the second and third dynodes. This conclusion is in an agreement with the results of afterpulse measurement obtained by Coates[7] for 8852 photomultiplier. However, no report has been made in literature on afterpulses which occurred in the 18-22 ns range after the main signal pulse. These pulses appeared at a lower rate but were consistently present in all three 8850s. Furthermore, the amplitude of these afterpulses was approximately one half of the single-photoelectron pulse amplitude, unlike those at 342-415 ns time range which were 3 to 4 times larger.

The afterpulses in the 18-22 ns range were the most probably generated by He^+ ions, which were in existance between the first and second dynode, striking the first dynode and causing the secondary emission. This conclusion is based on calculation of electron transit time betweeen the photocathode and the first dynode and the photomultiplier anode. Also the electric field distribution was taken into account. The 18-22 ns time range increased when the voltage between the photocathode and the first dynode/focusing electrode was decreased because of the change in the electric field intensity and distribution.

The experiment described above shows that 8850 photomultipliers have a long usable lifetime without serious increase in afterpulses in a typical laboratory environment. However, necessary corrections should be made in single photon counting systems to account for existance of afterpulses when accurate results from the fluorescence lifetime measurement are required. This is particularly important in experimental situations where lifetime measurements are made over a dynamic range of several decades.

ACKNOWLEDGMENTS

This work was performed as part of the program of the Electronics Research and Development Group of the Lawrence Berkeley Laboratory and was partially supported by the Director, Office of Energy Research, Office of High Energy Nuclear Physics, Division of High Energy Physics of the U. S. Department of Energy under Contract No. DE-AC03-76SF00098.

Reference to a company or product name does not imply approval or recommendation of the product by the University of California or the U. S. Department of Energy to the exclusion of others that may be suitable.

REFERENCES

1. C. C. Lo, B. Leskovar, Evaluation of the 8850 Photomultiplier with a Cesiated Gallium-Phosphide First Dynode, LBL Engineering Note, EE-1383, September 1971.

2. B. Leskovar, C. C. Lo, Performance Studies of Photomultipliers Having Dynodes with GaP(Cs) Secondary Emitting Surface, IEEE Trans. Nucl. Sci., NS-19, No. 3, pp. 58-62 (1972).

3. B. Leskovar and C. C. Lo, Single Photoelectron Time Spread Measurement of Fast Photomultipliers, Nucl. Instr. and Methods, Vol. 123, No. 1, pp. 145-160 (1975).

4. B. Leskovar, C. C. Lo, P. R. Harting, K. H. Sauer, Photon Counting System for Subnanosecond Fluorescence Lifetime Measurements, Rev. of Sci. Instr. 47, No. 9, pp. 1113-1121 (1976).

5. P. R. Hartig, K. H. Sauer, C. C. Lo and B. Leskovar, Measurement of Very Short Fluorescence Lifetimes by Single Photon Counting, Rev. of Sci. Instr. 47, No. 9, 1122-1129 (1976).

6. B. Leskovar, Photomultiplier Characteristics Considerations for the Deep Underwater Muon and Neutrino Detection System. Proc. of the 1980 Deep Underwater Muon and Neutrino Detection Signal Processing Workshop, A. Roberts, Ed. Published by Hawaii DUMAND Center, University of Hawaii, Honolulu, pp. 21-40 (1980).

7. C. C. Lo and B. Leskovar, Evaluation of the New Generation RCA 8854 Photomultiplier, IEEE Trans. Nucl. Sci. NS-29, No. 1, pp. 184-190 (1982).

8. G. A. Morton, H. M. Smith, R. Wasserman, Afterpulses in Photomultipliers, IEEE Trans. Nucl. Sci., NS-14, No. 1, pp. 443-448 (1967).

9. P. B. Coates, The Origins of Afterpulses in Photomultipliers, J. Physics D: Applied Physics, 6, pp. 1159-1166 (1973).

10. W. C. Paske, He^+ Afterpulse in Photomultiplier: Their Effect in Atomic and Molecular Lifetime Determinations, Rev. Sci. Instr. Vol. 45, No. 8, pp. 1001-1003 (1974).

11. D. F. Barllett, A. L. Duncan, J. R. Elliott, Afterpulses in a Photomultiplier Tube Poisoned with Helium, Rev. Sci. Instr. Vol. 52, No. 2, pp. 265-267 (1981).

Table 1. Anode Dark Pulse Count at Different Photoelectron Levels

Photomultiplier Serial No.	Dark Pulse Counts (cps)[a]												% of Dark Pulses from 2 to 16 Photoelectron Levels	% of Dark Pulses from 3 to 16 Photoelectron Levels
	Photo-electron Level	1/8	1	2	3	4	5	6	7	8	9	10		
S03674		234	125	13.3	10.7	8.9	7.6	6.4	5.1	3.8	2.7	1.5	5.6	4.6
S04424		204	97	10.3	8.4	6.6	5.4	4.4	3.2	2.2	1.5	.88	5	4
P37574		217	93	13	11.3	9.7	8.1	6.5	4.9	3.5	2.2	1.6	6	5.2

[a]Dark Pulse Summation is defined by $\sum_{N\ \text{Photoelectrons}}^{16\ \text{Photoelectrons}}$ = counts per second

where N = 1/8, 1, 2, ...10

Table 2. Signal Induced Anode Pulse Count Rate at Different Photoelectron Levels

Photomultiplier Serial No.	Induced Pulse Count (cps)[a]												% of Dark Pulses from 2 to 16 Photoelectron Levels	% of Dark Pulses from 3 to 16 Photoelectron Levels
	Photo-electron Level	1/8	1	2	3	4	5	6	7	8	9	10		
S03674		108K	64K	6.3K	2.2K	1.8K	1.6K	1.4K	1.2K	863	551	302	5.8	2
S04424		107K	62K	5.1K	2.1K	1.7K	1.2K	672	322	162	98	50	4.7	1.9
P37574		103K	63K	10.7K	5.3K	4.8K	4.4K	3.8K	3.1K	2.5K	1.8K	1.2K	10	5

[a]Anode Pulse Summation is defined by $\sum_{N\ \text{Photoelectrons}}^{16\ \text{Photoelectrons}}$ = counts per second

where N = 1/8, 1, 2, ...10

Table 3. Afterpulse Performance of 8850 Photomultiplier

		Photomultiplier Serial No. S04424			Photomultiplier Serial No. S03674			Photomultiplier Serial No. P37574		
	Measurement Time Interval	0-680ns	0.45-7 μs	4.5-68 μs	0-680ns	0.45-7 μs	4.5-68 μs	0-680ns	0.45-7 μs	4.5-68 μs
Afterpulse Count Rate (cps)	Single Photoelectron Pulse Freq.= 100 KHz	145 @ 18ns 111 @ 352ns 222 @ 404ns	b	b	171 @ 18ns 155 @ 351ns 310 @ 415ns	b	b	135 @ 22ns 169 @ 343ns 507 @ 400ns	b	b
	Single Photoelectron Pulse Freq. = 10 KHz	b	a	b	b	a	b	b	a	b
	Single Photoelectron Pulse Freq. = 1 KHz	b		a	b		a	b		a
	Three Photoelectron Pulse Freq. = 10 KHz	10 @ 19ns 49 @ 360ns 98 @ 404ns	a	a	5.8 @ 19ns 181 @ 350ns 362 @ 413ns	a	a	7 @ 22ns 274 @ 342ns 822 @ 399ns	a	a

a - Afterpulses were not observed
b - Measurement was not made due to a measuring system limitation

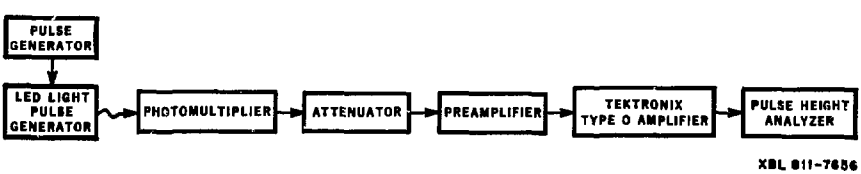

XBL 811-7656

Fig. 1 System block diagram for measuring pulse height spectrum.

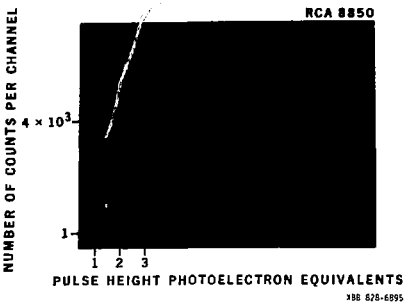

Fig. 2 Typical dark pulse height spectrum.

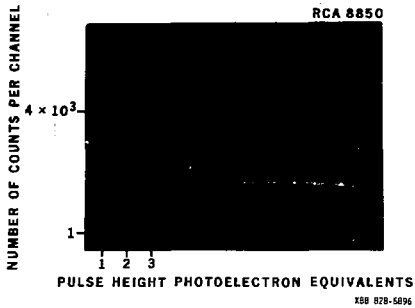

Fig. 3 Pulse height spectrum with 100 KHz signal induced count rate.

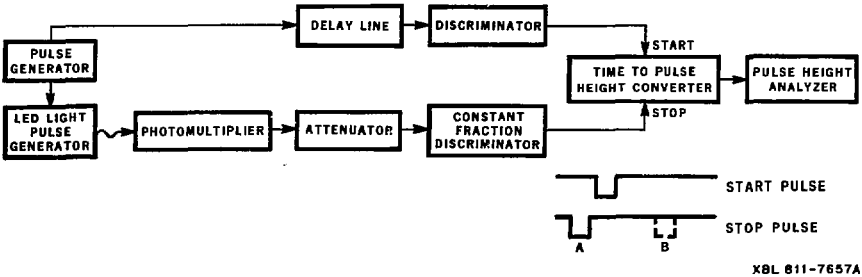

Fig. 4 System block diagram for measuring time spectrum of afterpulse.

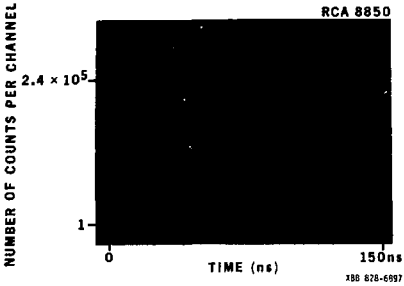

Fig. 5 Time spectrum of anode output pulse between 0-150 ns

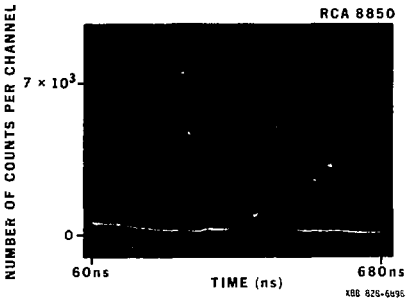

Fig. 6 Time spectrum of anode output pulse between 60 ns - 680 ns

LEGAL NOTICE

This book was prepared as an account of work sponsored by an agency of the United States Government. Neither the United States Government nor any agency thereof, nor any of their employees, makes any warranty, express or implied, or assumes any legal liability or responsibility for the accuracy, completeness, or usefulness of any information, apparatus, product, or process disclosed, or represents that its use would not infringe privately owned rights. Reference herein to any specific commercial product, process, or service by trade name, trademark, manufacturer, or otherwise, does not necessarily constitute or imply its endorsement, recommendation, or favoring by the United States Government or any agency thereof. The views and opinions of authors expressed herein do not necessarily state or reflect those of the United States Government or any agency thereof.

Lawrence Berkeley Laboratory is an equal opportunity employer.